Copyright Warning & Restrictions

The copyright law of the United States (Title 17, United States Code) governs the making of photocopies or other reproductions of copyrighted material.

Under certain conditions specified in the law, libraries and archives are authorized to furnish a photocopy or other reproduction. One of these specified conditions is that the photocopy or reproduction is not to be "used for any purpose other than private study, scholarship, or research." If a, user makes a request for, or later uses, a photocopy or reproduction for purposes in excess of "fair use" that user may be liable for copyright infringement,

This institution reserves the right to refuse to accept a copying order if, in its judgment, fulfillment of the order would involve violation of copyright law.

Please Note: The author retains the copyright while the New Jersey Institute of Technology reserves the right to distribute this thesis or dissertation

Printing note: If you do not wish to print this page, then select "Pages from: first page # to: last page #" on the print dialog screen

ABSTRACT

SURFACE PHENOMENA ON TIN-DIOXIDE POLYCRYSTALLINE LAYERS

by
Andrei A. Fluerasu

Polycrystalline tin-dioxide is widely used in the detection of reducing gases (such as H_2, CO, CH_4, C_2H_5OH,...) in air by measuring its conductivity changes. The advantage of gas sensors based on such sensing devices is low cost and high sensitivity. In contrast to their widespread applications and to their successful empirical research and development work, the present understanding of the chemical sensing mechanisms is still immature.

In this thesis, for gas sensors based on thick and porous tin-dioxide layers, a study of the response function upon variation of the partial pressure of ethanol vapors in 100% humidified air has been carried out. The influence of the working temperature and of the water vapors on the conductivity of the sensor was particularly emphasized.

Based on our experimental data, a theoretical model of the sensing mechanism in thick and porous tin-dioxide layers is presented. The model accepts the conduction mechanism as being governed by the Schottky potential barriers at the junction between grains. For describing the adsorption of gas molecules on the solid surface a method of "conditioned adsorption" was developed. The central idea was to assume that the reducing gas molecules are "adsorbed" (i.e. react) only on pre-adsorbed oxygen. The predictions made in the frame of our theoretical model are in good agreement with the experimental data.

SURFACE PHENOMENA ON TIN-DIOXIDE POLYCRYSTALLINE LAYERS

by
Andrei A. Fluerasu

A Dissertation
Submitted to the Faculty of
New Jersey Institute of Technology
in Partial Fulfillment of the Requirements for the Degree of
Master of Science

Department of Physics

October 1996

APPROVAL PAGE

SURFACE PHENOMENA ON TIN-DIOXIDE POLYCRYSTALLINE LAYERS

Andrei A. Fluerasu

Dr. Ken K. Chin, Thesis Adviser — Date
Professor of Physics, NJIT
Director, NJIT/Rutgers(Newark) joint Applied Physics M.S./Ph.D. Program

---

Dr. Kenneth R. Farmer, Committee Member — Date
Assistant Professor of Physics, NJIT

Dr. William N. Carr, Committee Member — Date
Professor of Physics, NJIT
Professor of Electrical and Computing Engineering, NJIT

BIOGRAPHICAL SKETCH

Author: Andrei A. Fluerasu

Degree: Master of Science

Date: October 1996

Undergraduate and Graduate Education:

- Master of Science in Applied Physics
  New Jersey Institute of Technology, Newark, NJ, 1996

- License in Physics
  University of Bucharest, Bucharest, Romania, 1994

Major: Applied Physics

ACKNOWLEDGMENT

The author wishes to express his sincere gratitude to his supervisor, Professor Ken K. Chin, for his guidance, friendship and moral support throughout this research. Many discussions regarding the conduction mechanisms, the nature of the surface Schottky barrier or the experimental results were very helpful.

Special thanks to Professors William N. Carr and Kenneth R. Farmer for serving as members committee.

The author is grateful to Professor K.R. Farmer for his continuos support throughout this research and particularly for the discussions about the adsorption of gaseous species on a solid surface which were of a real help.

And finally, a very special thank you to Professor Nicoale Barsan from the Institute of Physics and Technology of Materials, Bucharest, Romania currently at the Institute for Theoretical and Physical Chemistry, Tubingen, Germany. Professor Barsan was the first who guided the author in the area of surface phenomena at the gas-oxydic semiconductor interface. The devices which were studied in this work were realized under the guidance of professor Barsan two years ago. This research wouldn't have been possible without his continuos support.

TABLE OF CONTENTS

LIST OF TABLES

LIST OF FIGURES

Figure **Page**

CHAPTER 1

THE SEMICONDUCTOR SURFACE

The surface, defined as the interface between the lattice bulk and the ambient atmosphere, has a determined role in a large class of phenomena. Although the break of symmetry itself affects the structural properties of the bulk only for a few atomic layers, its influence on the electronic properties of the material can be extended in the volume.

1.1 Surface Sites & Surface States

Reconstruction and relocation in the lattice geometry cannot completely compensate the chemical bonds of the surface atoms. Therefore the surface atoms will have "dangling bonds" which are reflected by an increase in the chemical reactivity of those atoms. Foreign species can thus be bonded to the surface. A typical example for this phenomena is the growth of an oxide layer at the surface of a semiconductor.

In the case we are studying in the present work - the semiconducting ionic crystals placed in air - these "gas induced" surface states are predominant in comparison with the "intrinsic" Tamm states induced by the disturbance of the periodicity.

In terms of electronic band structure this increased reactivity is associated with the appearance of localized energy levels placed in the forbidden zone.

As an example of this approach, we will consider the case of the absorbed O^- ions at the surface of the tin oxide. Atomic oxygen ions (O^-) can exchange electrons with the semiconductor in accordance with the redox process such as

$$O^{2-} = O^{-} + e^{-} \qquad (1.1)$$

Both O^{2-} and O^{-} will be represented by the same surface state energy level. If the state is occupied by an electron, the species is the form O^{2-}, and if it is empty, the species is O^{-}. On the band diagram (Figure 1.1), the surface acceptor state O^{2-}/O^{-} is represented by an energy level E_t placed in the band gap.

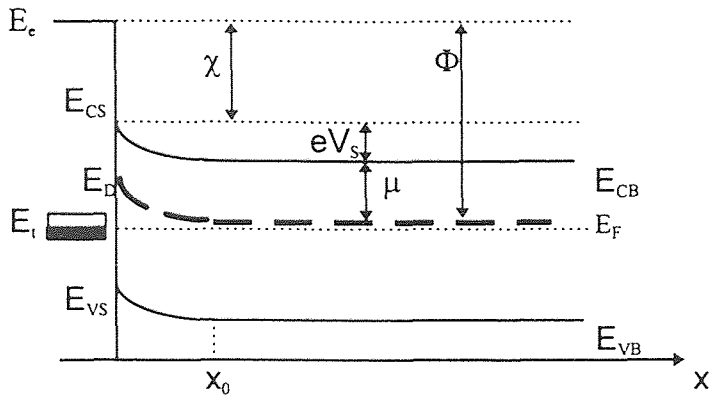

Figure 1.1 Surface Schottky-barrier profile with pinned Fermi level

In Figure 1.1 is shown also the Fermi level, E_F which is the electrochemical potential of electrons in the solid. The position of the surface state in the band gap determinates the band bending by the pinning of the Fermi level. (Figure 1.1). This effect will be studied in more detail in section 3 of this chapter.

1.2 Binding of Foreign Species to the Solid Surface

Another approach for describing the chemical and electronic behavior of the surface, complementary to the band model briefly emphasized in section 1, is an atomistic model. The atomic model is usually preferred in discussion of chemical processes at the solid surface, while the band model is usually preferred in discussion of electron exchange between the solid and the surface (Morrison, 1977). The two approaches are actually related and any picture of the complex phenomena occurring at the gas/solid interface should combine them.

In general, reactions between the absorbed species and the surface can be reversible or irreversible depending whether or not, new species appear at the surface. Adsorption is generally being classified into physisorption and chemisorption. The physisorption is realized without a true chemical bond between the adsorbate and the surface. Week, Van der Waals forces are at the origin of physisorption. Physisorption is a reversible process.

The chemisorption is associated with a stronger interaction between the adsorbate and the surface. Chemical reactions may occur at the surface causing the appearance of new species. Depending on the chemical reactions involved, the chemisorption, may be a reversible or an irreversible reaction. The growth of an oxide layer at the surface of a semiconductor is an example of an irreversible process which occurs at the surface. Examples of reversible reactions are reduction or oxidation of the sample, ion exchange, etc. Irreversible processes are unacceptable for practical gas sensing purposes, and such reactions must be avoided.

An useful tool for describing the interaction between a gas and a semiconductor is the quasichemical equation formalism (Barsan, 1993b) For exemplification, we will write the quasichemical equations describing the physisorption and the chemisorption of a species A on a adsorption center "S" from the surface of a solid.

$$A^{(g)} + S \underset{k_{-1}}{\overset{k_1}{\longleftrightarrow}} \begin{cases} A_S \\ A = S \\ A^+ - S^- \\ A^- - S^+ \end{cases} \qquad (1.2)$$

and the ionosorption of a species B;

$$B^{(g)} + S + e^- \underset{k_{-2}}{\overset{k_2}{\longleftrightarrow}} B_S^- \qquad (1.3)$$

An superscript (g) denotes a gaseous species while a subscript (s) denotes a surface - fixed species and k_1, k_{-1}, k_2, k_{-2} are reaction constants.

As it can be seen from the equation (1.2) the adsorption of the gaseous species A can be a simple physisorption (first case) or chemisorption, followed by the formation of a covalent bond (second case) or ionic bond (third and fourth case). Ionosorption of a species with lower electronic affinity than the adsorption center is described by the third case while ionosorption of a species with higher electronic affinity than the adsorption center is described by the last one.

In the equation (1.3), e^- represent a free electron from the conduction band. The equation describes in fact the adsorption of a species that has a higher electronic affinity

than that of the semiconductor. The B species is adsorbed on the free adsorption center and the chemical bond is realized with the capture of an electron from the conduction band. The B species ionosorption can also be done by the physisorption on a specific center "S_1":

$$B^{(g)} + S_1 \underset{k_{-3}}{\overset{k_3}{\longleftrightarrow}} B_{S_1} \qquad (1.4)$$

followed by the chemisorption, with the capture of a free electron, on another center "S_2":

$$B_{S_1} + S_2 + e^- \underset{k_{-4}}{\overset{k_4}{\longleftrightarrow}} B_{S_2}^- + S_1 \qquad (1.5)$$

By applying the mass-action law, one obtains the B adsorbed species concentration to the equations, one obtains from the equation (1.3), for the B absorbed species:

$$[B_S^-] = \frac{k_2}{k_{-2}} P_B [S] n_S \qquad (1.6)$$

and from equations (1.4) and (1.5):

$$[B_{S_2}^-] = \frac{k_3 k_4}{k_{-3} k_{-4}} P_B [S_2] n_S \qquad (1.7)$$

where P_B represents the partial pressure of the B species in the gaseous state, n_S represents the electronic concentration in the surface conduction band (that can take part in the reaction) and by "[ ]" we understand the superficial concentration of the specified gas.

We observe that for the equilibrium concentration (when the mass-action law can be applied) the relations described by (1.6) and (1.7) are the same.

The surface reactions can also be described by the quasichemical equations. The reaction which describes the ionosorption of a species B (by extracting an electron from the conduction band) followed by reaction with a species C, that comes from the ambient atmosphere is:

$$C^{(g)} + B_S^- \xrightarrow{k_7} CB^{(g)} + S + e^- \qquad (1.8)$$

As a result, the molecule CB is desorbed and the adsorption site S becomes free. Such type of reaction occurs at the surface of the tin-dioxide between reducing gas and chemisorbed oxygen. The reaction described by (1.8) is irreversible. Usually the adsorption of B cannot be done by adsorption of CB and dissociation of this one at the surface.

To determine the relations between the concentrations corresponding to the stationary state, a rate equation is used. From (1.3) and (1.8) we can deduce:

$$\frac{\partial[B_S^-]}{\partial t} = k_2 P n_S [S] - k_{-2}[B_S^-] - k_7 P_C [B_S^-] \qquad (1.9)$$

and for the stationary case we obtain:

$$[B_S^-] = \frac{k_2 P_B n_S [S]}{k_{-2} + k_7 P_C} \qquad (1.10)$$

In this equation, $[B_s^-]$, $[P_B]$ and $[S]$ are not independent. Defining $[S_t]$, the total concentration of adsorption sites (occupied or empty), we have:

$$[S_t]=[S]+[B_S^-] \qquad (1.11)$$

Thus, the equation (1.10) becomes:

$$[B_S^-] = \frac{k_2 n_S P_B [S_t]}{k_{-2} + k_7 P_C + k_2 P_B n_S} \qquad (1.12)$$

We define the coverage ratio:

$$\theta = \frac{[B_S^-]}{[S_t]} \qquad (1.13)$$

From equations (1.12) and (1.13) we obtain, for the coverage ratio:

$$\theta = \frac{1}{1 + \frac{k_7 P_c + k_{-2}}{k_2 P_B n_s}} \qquad (1.14)$$

The influence of various parameters on the adsorption appears clearly from this equation:

The decrease of the coverage ratio "θ" value is determinate by:

- high values for k_7, which describes the elimination of the B species from the surface by the reaction with the C species
- high values for k_{-2}, which describes the B species elimination from the surface by the desorption.

The increase of the "θ" value is determinate by:

- large values for k_2, which describes the B species absorption in gaseous phase.
- large values for P_B and n_S, as parameters that influence the absorption.

One can easily see from equation (1.14) that for $k_7P_C/k_{-2} << 1$, the species C will not have a noticeable effect on the adsorption. This happens if the desorption of B dominates the desorption by interaction with C.

On the other hand side, if $k_7P_C/k_2P_Bn_S >> 1$, the species B is completely eliminated from the surface by reaction with C and desorption of CB.

This approach allows us to have a relation in between the partial pressure of a reducing gas and the coverage ratio of O^- ions, which is an important parameter that influences the conductivity.

The relation (1.14), though, introduces the parameters k_7, k_{-2}, k_2 which cannot be determined but by fitting with experimental data. In the next section we will introduce a statistical physics model of the adsorption at a solid surface which will allow us to reduce the number of parameters.

1.3 Adsorption

In this section, a model of the adsorption of a gaseous species on a solid surface is presented. The coverage ratio of the adsorbed species (surface concentrations of adsorbate per surface concentration of adsorption sites) will be deduced as a function of the gas pressure, the surface concentration of the adsorption sites, the energy of the adsorbate when fixed at the surface and of course, the temperature. The result is a Langmuir-type isotherm. Based on this model, a method of "conditioned adsorption" will be developed in the next chapter for describing the interaction of the SnO_2 surface with atmospheric oxygen and with reducing gases.

1.3.1 The Model

The surface has a number of M adsorption sites. Molecules of a gas in contact with the surface may be adsorbed on those sites. We shall consider the mono-site partition function as 1 if the site is unoccupied and as $e^{-\beta\varepsilon}$ if the surface site is occupied. The energy ε introduced here is the adsorption energy of the adsorbed molecule. Internal degrees of freedom are neglected. If n is the number of adsorbed molecules (ranging from 0 to M), the grand-partition function of the two-dimensional surface gas may be written:

$$\Xi(\mu,T,M)=\sum_{n=0}^{M}\frac{M!}{n!(M-n)!}e^{-n\beta\varepsilon}e^{n\beta\mu} \qquad (1.15)$$

The surface which is in grand-canonical conditions, is in equilibrium with the gas. At equilibrium the chemical potentials of the gas and the surface are equal. The gas is assumed to be ideal and thus, the chemical potential is given by (McQuarrie, 1987):

$$\mu(T)=kt\ln\left(\frac{p}{\Pi}\right) \quad where \quad \Pi=\left(\frac{2\pi mkT}{h^2}\right)^{3/2}kT \qquad (1.16)$$

If N molecules of gas are adsorbed on the solid surface *(N<M)*, the coverage ratio is defined to be:

$$\theta=\frac{N}{M}$$

1.3.2 Adsorption Isotherms

For the 2-D gas, adsorbed on the solid surface, which is assumed to be a grand-canonical ensemble, we can write the thermodynamic properties as function of the grand-partition function:

$$pV=kTln\Xi$$

$$d(pV)=SdT+Nd\mu+pdV$$

For the number of adsorbed molecules, N, one can write:

$$N=\frac{\partial(pV)}{\partial\mu}=kT\frac{\partial(\ln\Xi)}{\partial\mu}$$

By using (1.15), one can obtain, after simple manipulations:

$$N=\frac{Me^{-\beta(\varepsilon-\mu)}\sum_{n=0}^{M-1}\frac{(M-1)!}{(n-1)!(M-n)!}[e^{-\beta(\varepsilon-\mu)}]^{n-1}}{\sum_{n=0}^{M}\frac{M!}{n!(M-n)!}[e^{-\beta(\varepsilon-\mu)}]^{n}}=M\frac{e^{-\beta(\varepsilon-\mu)}}{1+e^{-\beta(\varepsilon-\mu)}}$$

It is convenient to introduce, instead of ε, a numeric parameter ρ, defined by the following relation:

$$\varepsilon=-kT\ln\rho \qquad (1.17)$$

By using the expression for the chemical potential of the ideal gas (1.16) the coverage ratio becomes:

$$\theta = \frac{N}{M} = \frac{\rho\left(\frac{p}{\Pi}\right)}{1 + \rho\left(\frac{p}{\Pi}\right)} \qquad (1.18)$$

1.4 Space Charge Effects

Formation of electric charge double layers is a common occurrence at a solid state surface. For example, an adsorbed charged sheet of oxygen ions, on a metallic surface will induce such double layers. The oxygen has a large negative net charge, therefore, a equal opposite positive charge will be induced on the metallic surface. A first approximation of this double layer consists in two charged planes (Figure 1.2)

O^-	O^-	O^-	O^-	O^-
M^+	M^+	M^+	M^+	M^+
M	M	M	M	M

Figure 1.2 Dipolar sheet at a metallic surface

The potential V, must, of course, obey the Poisson equation.

$$\frac{d^2V}{dx^2} = -\frac{\rho}{\varepsilon} \qquad (1.19)$$

The solution of this one dimensional equation, with the appropriate boundary conditions: $V(x=o)=V_s$ and $V(x=x_0)=0$ (x_0 is the width of the dipole sheet and V_s the potential at the surface) leads to a simple solution which is represented in Figure 1.3

According to Gauss law, the potential can be written as a function of the surface charge density:

$$V(x)=\begin{cases} 0, & x<0 \\ \frac{\sigma}{\varepsilon}x, & x\in(0,x_0) \\ \frac{\sigma}{\varepsilon}x_0, & x>x_0 \end{cases}$$

Thus, for the barrier height, V_s, we have the formula:

$$V_s=(\sigma x_0)/\varepsilon$$

We can estimate now the surface barrier induced by an adsorbed monolayer of oxygen ions on a metallic surface. A typical value for the surface density of atoms for an arbitrary crystallographic plane is of $2*10^{19}$ atoms/m^2. A reasonable value for x_0 is around 3 to 10Å, and for the relative dielectric constant, of 10.

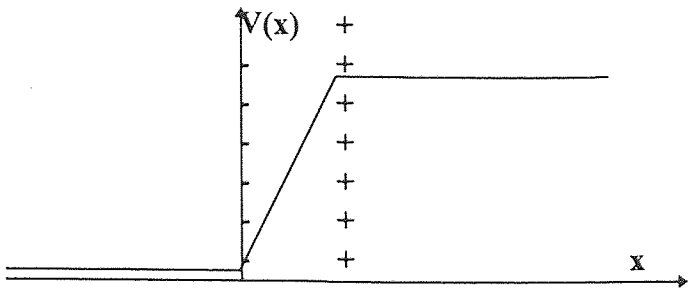

Figure 1.3 Potential barrier across a dipolar sheet

With these data, a value of 3.5V is obtained for V_s. This is an extremely high value for a surface barrier. A more realistic model takes into consideration a space distribution of the positive charge induced by the adsorbed negative surface charge. The space charge density is no longer zero in this case. Further on, we shall consider the space-charge region which occurs at the surface of a semiconductor. Surface states can be present at the semiconductor surface. Charge carriers may be trapped on these surface states (acceptor-like) or may be injected from those states (donor-like). Depending on the type of the surface states (donors or acceptors) and of the conductivity type of the semiconductor, three types of space-charge layers may appear below the surface. The Figure 1.4 presents for the three different space-charge types (depletion, accumulation and inversion) the band structure and the carrier concentrations for an n-type semiconductor. Similar figures can easily be drawn for a p-type semiconductor too. The quantitative description of these phenomena can be done by solving the Poisson equation with the appropriate boundary conditions and imposing the global neutrality condition for the semiconductor.

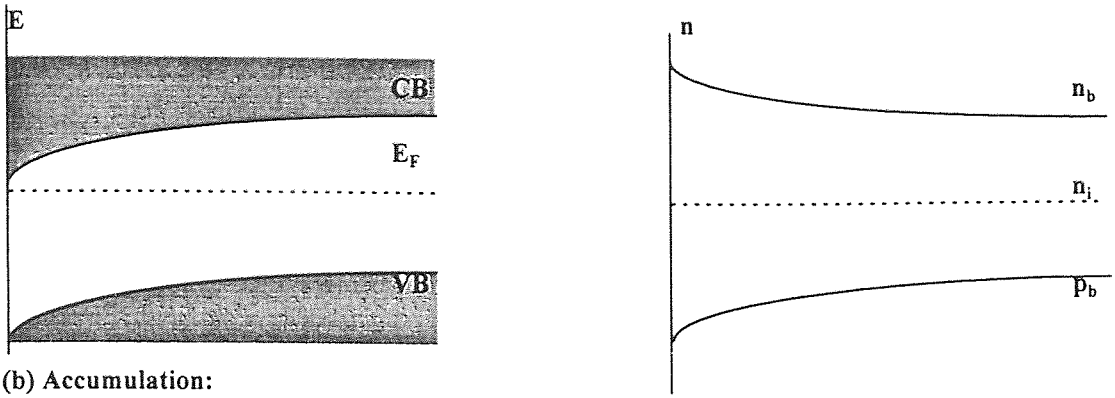

(b) Accumulation:
The presence of donor states at the surface creates an excess of majority carriers in a layer below the surface. The surface will acquire thus, a net positive charge and this will cause an downward band bending

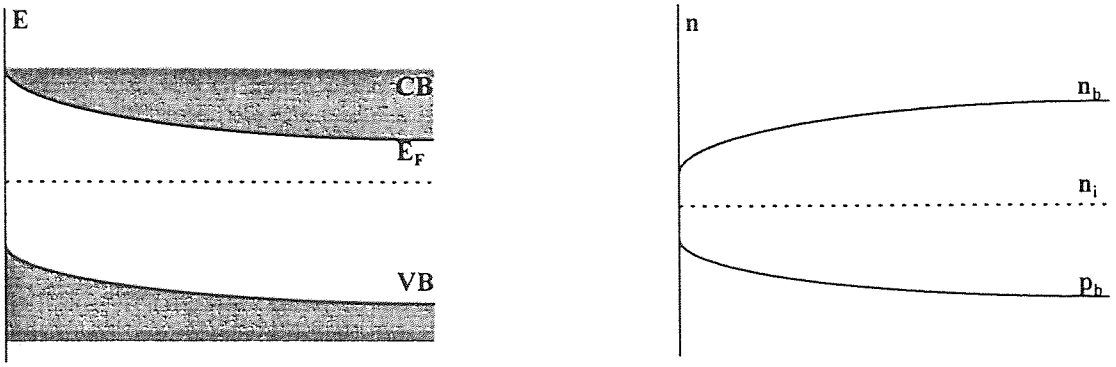

(a) Depletion:
Occupied electron-accepting states on the surface of an n-type semiconductor deplets a layer below the surface. The space charge consists basically in immobile ion cores. The net negative charge from the surface causes an upward band bending

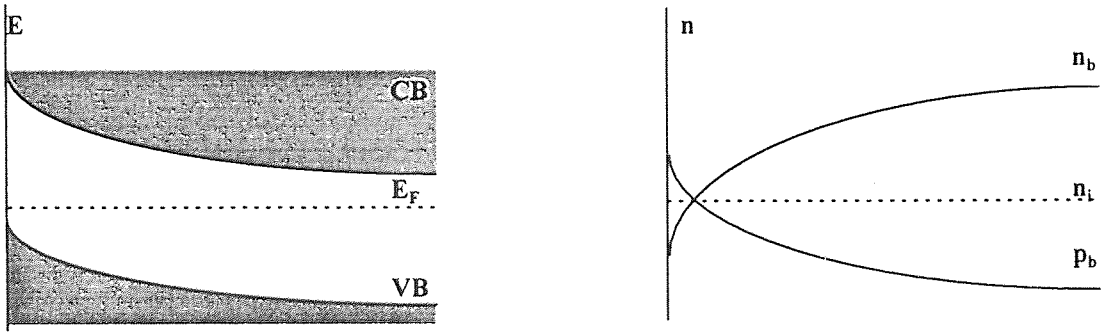

(c) inversion:
The mechanism is the same as for depletion layers. The trapped surface charge become that large in this case that in the space charge region, below the surface, the number of minority carriers will exceed that of majority carriers

Figure 1.4 Space charge layers at a n-type semiconductor surface

We will find the concentration of majority carriers and the band-bending function of the Schottky barrier for an n-type semiconductor with acceptor surface states (electron traps), using the completely depleted space-charge layer model.

The assumptions of this model are:

- The concentration of minority carriers (holes) can be neglected
- The concentration of majority carriers is so small in the space-charge layer that it can be neglected too. In other words, the model assumes that the surface traps are creating a charge layer just below the surface which is completely depleted of conduction electrons
- All the donors are ionized

The general expression for the charge density in the semiconductor bulk is:

$$\rho=(N_D-N_A+p-n)e \qquad (1.20)$$

where, n is the free electron concentration, p the hole concentration, N_D and N_A are the concentration of ionized donors and acceptors respectively.

If n_b is the bulk electron concentration, the charge density in the space-charge layer becomes, in the limits of the Schottky model:

$$\rho=N_D e= n_b e \qquad (1.21)$$

From the neutrality conditions one can deduce the surface charge density:

$$\sigma=-\rho x_0 \qquad (1.22)$$

The boundary conditions imposed by the Gauss' Law are:

$$\left.\frac{dV}{dx}\right|_{x=0} = -\frac{\sigma}{\varepsilon} \quad , \quad \left.\frac{dV}{dx}\right|_{x=x_0} = 0 \qquad (1.23)$$

The Poisson equation (1.19) with the space charge density given by (1.21) and the boundary conditions (1.23) has the solution:

$$V(x) = -\frac{en_b}{2\varepsilon}x^2 + \frac{en_b}{\varepsilon}xx_0 + V_0$$

By choosing a convenient value for the additive constant V_0, one gets:

$$V(x) = -\frac{en_b}{2\varepsilon}(x - x_0)^2 \qquad (1.24)$$

This formula applies for the space charge region, namely, for $x \in (0, x_0)$

The band bending function *W(x)* is defined to be:

$$W(x) = \frac{e^2 n_b}{2\varepsilon}(x - x_0)^2 \qquad (1.25)$$

The potential barrier height is $V_s=V(x_0)$:

$$V_S = \frac{en_b}{2\varepsilon} x_0^{\,2} = \frac{\sigma^2}{2\varepsilon n_b e} \tag{1.26}$$

We define the Debye length:

$$\lambda_D = \left(\frac{\varepsilon kT}{e^2 n_b} \right)^{1/2} \tag{1.27}$$

One can redefine then the band-bending function by using the Debye length:

$$W(x) = \frac{kT}{2} \left(\frac{x - x_0}{\lambda_D} \right)^2$$

The equation (1.25) is a good approximation of the band bending function as it can be seen from the results of Frankl (Frankl, 1967) who compared the band bending functions obtained by the numerical integration of the Poisson equation, with the charge density given by (1.20) with the function obtained from the model of complete depleted charge layer (1.25). By using this model we have derived a value for the Schottky surface barrier height as a function of the surface charge density. The height of surface potential barriers controls the conduction mechanism for thick and porous tin-dioxide layers. Basically, if the material consists in grains with sizes comparable to the Debye length, the conduction mechanism is that of tunneling through the potential barrier which occurs at

the contacts between grains. The Debye length gives an order of magnitude of the penetration depth of the band-bending function. For materials with dimensions much larger that the Debye length, the influence of the surface on the electronic properties is hindered by the bulk. If the size of the semiconductor is much smaller than the Debye length, then the influence of the surface is important but due to the fact that energy bands are almost "flat" the conduction is not any more governed by the Schottky barriers. The case studied in this work is that of thick and porous tin-dioxide sensors with grain sizes comparable to the Debye length.

CHAPTER 2

NON-EQUILIBRIUM PHENOMENA AT THE TIN DIOXIDE-GAS INTERFACE

Polycrystalline tin-dioxide (SnO_2) layers are widely used in the detection of reducing gases (such as H_2, CO, CH_4, C_2H_5OH,...) in air by measuring conductivity changes. The advantage of gas sensors based on such sensitive layers is low cost and high sensitivity for temperatures starting from the room temperature, and this has made them very useful devices.

2.1 Interaction with Gases at the SnO_2 Surface

Tin Dioxide (SnO_2) is a wide band-gap semiconducting ionic crystal. Its crystalline structure is the same as that of the rutillum (Figure 2.1) The forbidden energy gap is of 3.6eV (Kohnke, 1962). Without any intended doping the SnO_2, has an n-type conductivity which is associated with the oxygen bulk vacancies.

The surface oxygen vacancies play the role of chemisorption sites for atmospheric oxygen. Their surface concentration N_S can be evaluated by considering that the bulk oxygen vacancies actually are within a sheet of thickness on the order of magnitude of the lattice constant (Barsan, 1994).

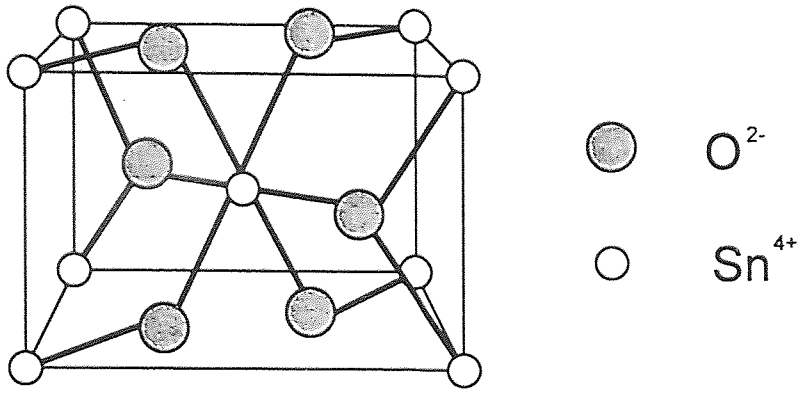

Figure 2.1 Crystalline structure of SnO_2

The deviation from stoichiometry was initially proved by measurements of the electrical conductivity at high temperatures as a function of oxygen partial pressure. (Maier and Gopel, 1988). Experimentally, a dependence of the conductivity on the oxygen partial pressure P_{O2} has been found following the empirical equations:

$$\sigma = C P_{O_2}^{-1/6} \qquad (2.1)$$

or:

$$\sigma = C P_{O_2}^{-1/4} \qquad (2.2)$$

as a function of the working temperature and of oxygen partial pressure. A dependence described by (2.1) can be obtained from the quasichemical equations formalism by considering the donor midgap states as being due to the oxygen vacancies. The dependence (2.2) corresponds to the presence of some acceptor impurities which are

compensating the donors. The presence of Fe and Al has been proved by elemental analysis.

Singly and doubly ionized vacancies, acting as donors, induce allowed energy levels in the band-gap, situated at 0.034eV and 0.15eV respectively from the conduction band edge (Jarjebski and Marton, 1976). Adsorbed oxygen (neutral O_2, singly ionized molecular ions O_2^-, and singly and doubly ionized O^- O^{2-} ions) act as surface acceptors (traps) by binding electrons. The effect is a decrease in the surface conductivity. For pure materials, the electrical characteristics are presented in Table 1 and Table 2.

Table 1 Net donor concentration and ionization energies
(after Barsan, 1993b)

N_D-N_A (m^{-3})	E_D (meV)
$9{,}2*10^{21}$	34, 140

Table 2 Concentrations and ionization energies of donors and acceptors
(after Barsan, 1994b)

N_D (m^{-3})	N_A (m^{-3})	E_{D1} (meV)	E_{D2} (meV)	E_A (meV)
$2.5002*10^{22}$	$5*10^{21}$	40	140	780

The adsorption of oxygen was described (McAllen et al. 1987) by the following kinetic scheme (e represents an electron, R, a reducing gas molecule):

$$O_2^{gas} \leftrightarrow O_2^{ads} \xleftrightarrow{e} O_2^- \xleftrightarrow{e} O^-$$
$$O^- \xleftrightarrow{e} O^{2-}$$
$$O^- \xleftrightarrow{H_2O} 2OH^-$$
$$O^- \xleftrightarrow{R} RO$$

The law of mass action applied to each step of the general scheme yields the steady state occupancy for the different oxygen surface states. The interaction of oxygen and water vapors with the tin oxide surface was experimentally studied by Yamazoe (Yamazoe, 1979) by Temperature Programmed Desorption (TPD). The results obtained are presented in table 3. In parenthesis are marked the temperatures from which the respective species has a desorption maximum. Effects on the electrical conductance and the coverage ratio are also presented. The coverage ratio is the ratio between the number of chemisorbed oxygen ions and the number of Sn atoms. The (110) plane was exposed to the oxygen atmosphere.

Table 3 Characteristics of interaction between the SnO_2 and permanent atmospheric gases. (after Barsan, 1993b)

Gas	Species (Tm)	ΔG (adsorbtion)	ϑ (%)
O_2	O_2^- (80 °C)	has no effect	0.021
	O^- (150 °C)	decrease in cond.	0.022
	O^{--} (500 °C)	decrease in cond.	0.79
H_2O	H_2O (110 °C)	has no effect	4.5
	-OH (400 °C)	increases the cond.	15.0

Two mechanisms are proposed by Heiland and Kohl (Barsan, 1993b) for the way in which the chemisorbed hydroxyl increases the conductivity.

- A donor (O_0H group) is obtained by the following reaction scheme:

$$H_2O + Sn_{Sn} + O_0 \underset{k_{-4}}{\overset{k_4}{\longleftrightarrow}} HO - Sn_{Sn} + O_0H$$

$$O_0H \underset{k_{-5}}{\overset{k_5}{\longleftrightarrow}} O_0H + e^-$$

- The resultant donor is, in this case, an oxygen vacancy. The quasichemical equations describing this process are:

$$H_2O^{(g)} + 2Sn_{Sn} + O_0 \underset{k_{-6}}{\overset{k_6}{\longleftrightarrow}} 2(HO - Sn_{Sn}) + V_0$$

$$V_0 \underset{K_{-7}}{\overset{k_7}{\longleftrightarrow}} V_0^{++} + 2e^-$$

In all these equations, a subscript 0 denotes a surface-fixed species on a oxygen vacancy, and a subscript Sn denotes a surface-fixed species on a Sn atom. The chemisorption of the OH group at the semiconductor surface is an example of localized chemisorption (chemical bond where no free bulk charge carriers are participating). Due to the high electron affinity of the hydroxyl, the OH-Sn group has a dipole character. The presence of these dipoles at the semiconductor surface changes its characteristics.

It can be seen from above that the water vapors have an important role in the chemical reactions which occur at the semiconductor surface. The effect of the vapors is the same as the effect of a reducing gas i.e., causes an increase of the conductivity. Thus,

the water vapors themselves act as a "parasite" gas and this makes the problem of determining the presence and measuring the pressure of a specific gas to be even more complicated, as it is difficult to control a stable atmosphere (humidity) in real working conditions.

An oxide semiconductor sensor detects a reducing gas by monitoring changes in electrical conductivity of a polycrystalline element, which, in the case of a commercial SnO_2 sensor, can comprise in addition to the SnO_2 crystallites, also Al_2O_3 (binder), Pt(sensitizer), Pd(sensitizer), etc. Generally speaking, a semiconductor gas sensor consists of two functions: (Yamazoe, 1991)

- A "receptor function" which identifies or recognizes a chemical substance. Basically this is a chemical function, reflected in the case of the SnO_2 sensors by the chemical reactions which occur at the semiconductor surface with reducing gas molecules.
- A "transducer" function, which converts the chemical signal into an output, electrical signal. The tin oxide sensors are detecting the reducing gases by monitoring changes in conductivity.

In the range of temperatures in which SnO_2-based gas sensors work (300K-700K), the chemical sensing mechanism is the surface reaction between chemisorbed oxygen on the surface oxygen vacancies and a reducing gas. The detection of gases on such layers is done in two steps. First, the oxygen is chemisorbed as charged species (O_2^-, O^-, O^{2-}), and this induces the appearance of a surface depletion layer of lower conductivity. The effect of the reducing gas consists in a decrease of the concentration of chemisorbed oxygen, by means of chemical interaction with this one, which causes an increase of the conductance.

Some of the conclusions for which there are experimental evidence and that are generally accepted in literature are (Barsan 1993b):

- For the working temperature range (300K-800K), the reaction between SnO_2 and the reducing gas is a surface reaction.
- There are reducing gases (CO for example) which interact only with chemisorbed oxygen. Therefore the detection of these gases is possible only in the presence of the oxygen in the atmosphere.
- There are reducing gases (such as H_2, CH_4) which can interact with the surface lattice oxygen
- The chemisorbed oxygen species are: O_2^-, O^-, O^{2-}
- The interaction with the reducing gas causes a global increase of the conductivity of the sensor
- The relation between conductivity and partial pressure of the reducing gas for a wide range of pressures (10 ppm - 10^4 ppm) is:

$$G = G_0 \cdot P_R^{\,n} \quad n \in (0.2,1)$$

The sensitivity and selectivity of gas sensors based on such oxide semiconductor layers is basically determined by several factors. The extent of the space-charge layer is an important one (Mizsei, 1995). This depends, as we have seen in Chap. 1 on the Debye length:

$$\lambda_D = \left(\frac{\varepsilon \varepsilon_0 k_B T}{q^2 n_b} \right)^{1/2}$$

If the dimensions of the SnO_2 film (thickness of a thin SnO_2 film, or grain sizes of a thick and porous SnO_2 film) is of the order of the Debye length (or less than it), then the surface effects are noticeable and this makes possible the gas detection. One other important factor which determines the sensitivity is the working temperature. Usually, for a specific gas there is a range of temperatures, where the materials are sensitive to this particular gas. Chemical methods for improving the sensitivity of such materials, are also available. One of the most popular is the surface doping with catalitically active materials such as Pt or Pd (Mizsei, 1995)

In spite of their advantages, there are also problems, which, at least until now, hinder their use as measuring devices. Lack of stability - i.e. dependence of ambient atmosphere conditions (humidity is a important factor) and on "aging" and poor selectivity for different reducing gases are most serious. Calibration curves for SnO_2-based gas sensors can be obtained, but only for high-enough partial pressures of the gas. (Barsan, 1994a) Humidity also has a very important role in the response of the sensor. Therefore, the sensor response (conductivity), in general is not a state function in a thermodynamic sense (or at least there are missing parameters!)

2.2 Tin Dioxide Based Gas Sensors

Solid state gas sensors based on SnO_2 have become predominant solid-state devices for gas detection used in domestic, commercial and industrial premises. A huge variety of

ceramic, thick-film and thin-film devices has been developed over the years with mostly an empirical optimization of their performances. As a general rule for gas sensing devices, any kind of SnO_2 sensor must operate under conditions in which the overall conductivity is influenced by surface phenomena such as adsorption.

The most important factors influencing the sensitivity of such devices to the presence of a reducing ambient gas are, the quality of the semiconductor surface, the presence of catalytically active materials at the semiconductor surface, the porosity of the material. (Gopel, 1995) For thick and porous sensing layers, the influence of the surface on the electrical properties is important if the dimensions of the crystallites are comparable with the Debye length. As seen in section 1.4, the Debye length, which is given by the equation (1.27) is a measure of the penetration depth of the band bending due to the adsorbed charged species (O^- in this particular case) in the bulk. It is natural to assume that the electrical properties of the material are dramatically perturbed if the band bending occurs for depths comparable to the physical dimensions of the grains thus the electron concentration is highly perturbed.

The influence of the particle sizes and of the contacts on the band structure of the sensing material is schematically presented in Figure 2.2. Besides the preparation of the long-term stable SnO_2 grain structure, the geometry of contacts is of a particular importance in the design of both thin-film and thick-film gas sensors. (Gopel, 1995)

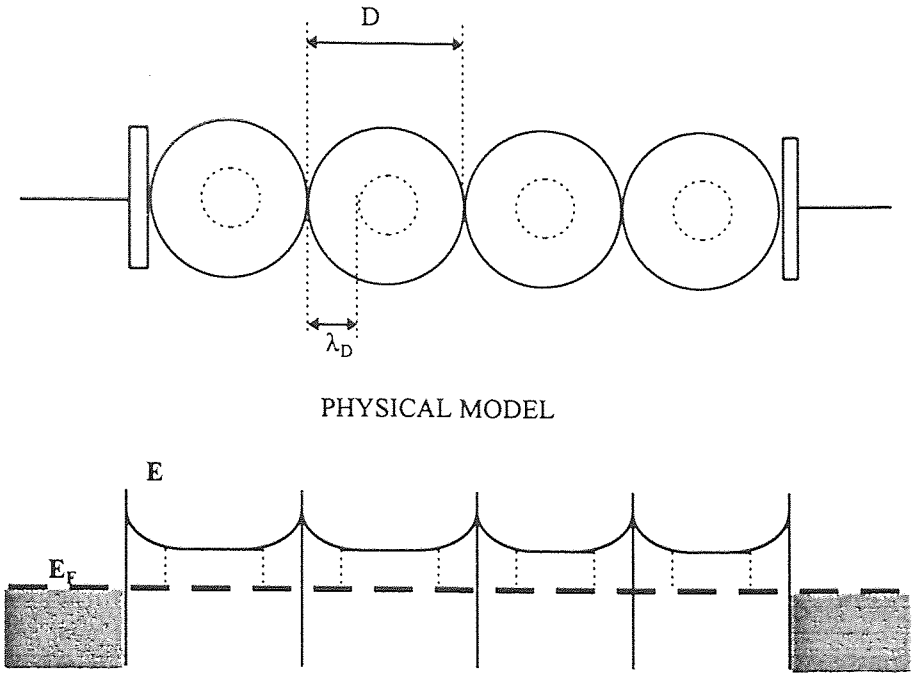

(a) The Debye Length is smaller than the grain size

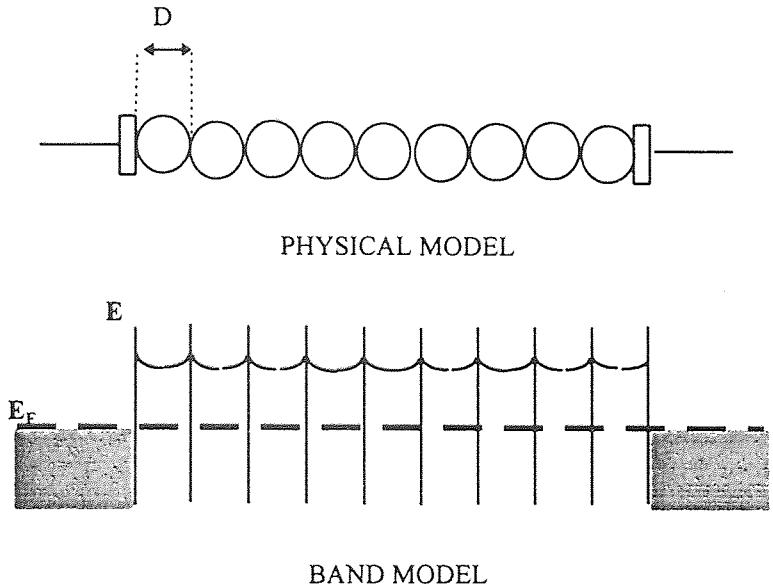

(b) The Debye Length is comparable or larger than the grain size

Figure 2.2 Influence of particle sizes and contacts on the band structure.

Sensitivity and selectivity of tin oxide based gas sensors is improved by means of several methods, out of which one of the most popular is the surface doping with catalytically active metals (Pt or Pd usually). The two mechanisms usually considered in the literature for the influence of the dopants, are the spill-over and the Fermi level mechanism. (Yamazoe, 1991), (Morrison 1987). In the spill-over the surface dopant increases the rate of chemical processes leaving the sensing mechanism essentially the same. In the Fermi energy control mechanism, the dopants change the electrostatic potential due to their different electronic affinities. The conductivity varies with the Fermi level pinning according to the Fermi level of the dopants. The theoretical study of the mechanism in which surface catalyst affects the intergranular region is not the aim of this work. Some experimental data will be presented to illustrate the influence of metallic Pt and Pd dopants on the DC conductivity of SnO_2 sensors.

2.2.1 Thick Film Gas Sensors

Thick film SnO_2-based gas sensors were tested in ethanol (C_2H_5OH) atmospheres. Classical Taguchi type sensors, consisting of a ceramic tube (alumina) with a platinum heater inside on which a thick gas-sensing tin dioxide film was printed, was chosen. The material was prepared by a wet chemical method (Schweizer-Berberich et al., 1996). First $Sn(OH)_4$ was precipitated by adding ammonia to an aqueous $SnCl_4$ solution. Tin dioxide with different grain sizes was obtained by controlling annealing (4-15 h) at elevated temperatures (450, 800 and 1000 °C). The solvent (1,3-propane-diol) was burned out at 700°C for 5 min. This second temperature treatment does not influence the grain size (Schweitzer-Berberich et al., 1996). The surface doping was performed by a powder

impregnation using Pt and Pd chlorides for 20 h at room temperature. The doped powders were annealed again at 450°C for 1-4 h in order to convert the chloride to metal (or metal oxide). The concentration of the dopants in the tin dioxide powder was 0.2% wt. The thickness of the ceramic materials were between 0.1 and 1 mm

Conductance and time of response upon variation of the concentration of ethanol (C_2H_5OH) and as a function of the working temperature were measured by means of a very simple electrical circuit. A load resistor R_L was connected in series with the sensor and a d.c. voltage source (V). The voltage V_{RL} across the load resistor R_L was monitored on a Y-t recorder. By measuring this voltage one find for the conductance of the sensor:

$$G = \frac{V_{RL}}{R_L\left(V - V_{RL}\right)}$$

The desired C_2H_5OH concentrations were achieved by using the equilibrium atmosphere of ethanol aqueous solutions. Their alcoholic concentrations were: 0, 0.005, 0.015, 0.025 and 0.040 vol. %; 0.25 l of the above mentioned solutions were introduced in 2l Erlenmeyer flasks which were closed with corks. The sensors were successively introduced in increasing ethanol concentrations. In Figure 2.3 a typical variation of the voltage across the load resistor when the sensors is exposed at increasing ethanol-containing atmospheres is presented. An SnO_2 sensor, formed at 800°C was successively introduced in the vessels containing the prepared atmospheres. The working temperature was of 250°C and the ambient temperature of 25°C. The sequence of atmospheres were: clean air 30% relative humidity (ambient atmosphere); clean air 100% relative humidity;

142 ppm ethanol; 428 ppm ethanol; 714 ppm ethanol; 1143 ppm ethanol; clean air 30% relative humidity. The relative humidity for all ethanol-containing atmospheres was 100%

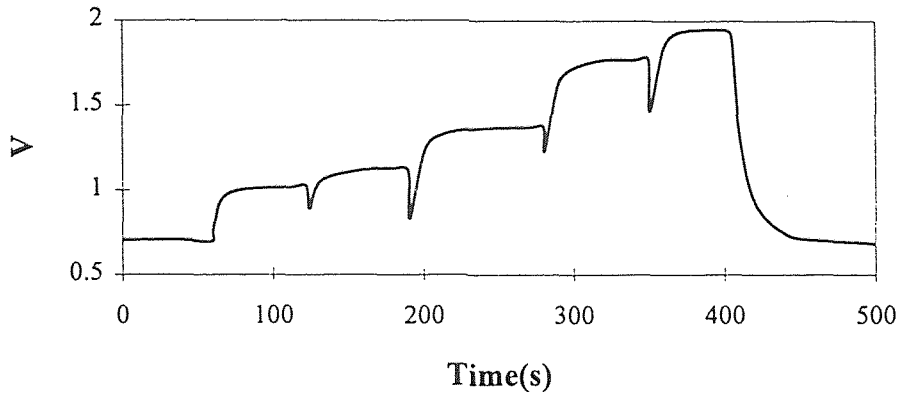

Figure 2.3 Voltage across the load resistor as a function of time

All the sensors were tested in this way. This allowed us to estimate when an equilibrium state is reached and to evaluate the time of response also. The pressure of the equilibrium atmosphere was atmospheric and the temperature ranged from 22 to 26 °C. The vapor concentrations of C_2H_5OH were calculated using the Dubrowski formula (Barsan, 1993a). The working temperature of the sensors ranged from 150 to 450°C.

Several types of sensors were tested. They were SnO_2, SnO_2-Pt and SnO_2-Pd sensors with average grain sizes between 10 nm and 30 nm corresponding to a 450°C annealing temperature and pure SnO_2-based sensors with average grain sizes of 30-70 nm corresponding to an 800°C annealing temperature. The aim of this section is to describe

the behavior of these sensors in atmospheres containing ethanol and water vapors (100% relative humidity). The influence of the working temperature, the grain size and the dopants will be emphasized.

The influence of the metallic dopants on the ethanol-sensing properties was studied by measuring the conductivity and the time of response of pure and doped sensors with same average grain sizes (annealed at 450°C). The ratio of the conductance G in humidified (100%) ethanol-containing atmospheres and the conductance G_0 in clean, 100% humidified air is presented in Figure 2.4. With respect to the pure SnO_2 sensor, one can observe an increase of the sensitivity of the SnO_2-Pt sensor and a decrease of the sensitivity of the SnO_2-Pd sensor. The maximum sensitivity is obtained, for the SnO_2 sensor for a 300°C working temperature for ethanol concentrations exceeding 300 ppm and for a 250°C working temperature at gas concentrations lower than 300 ppm. The maximum sensitivity for the SnO_2-Pd sensor for concentrations exceeding 500 ppm is still achieved for a 300°C working temperature, though at concentrations lower than 500 ppm, a higher working temperature, of 350°C is needed to achieve the maximum sensitivity. Thus, though the conductance itself may have a large variation, the sensitivity (G/G_0 ratio) for ethanol, doesn't varies dramatically if one use surface-doped SnO_2. The performances of SnO_2-Pd sensors are enhanced, in the sense that the sensitivity is higher and the optimal working temperature is lower.

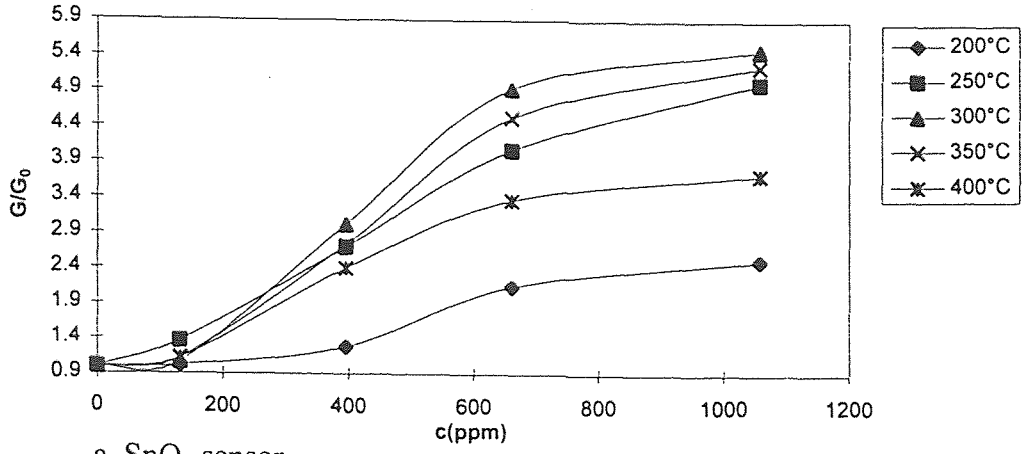

a. SnO_2 sensor

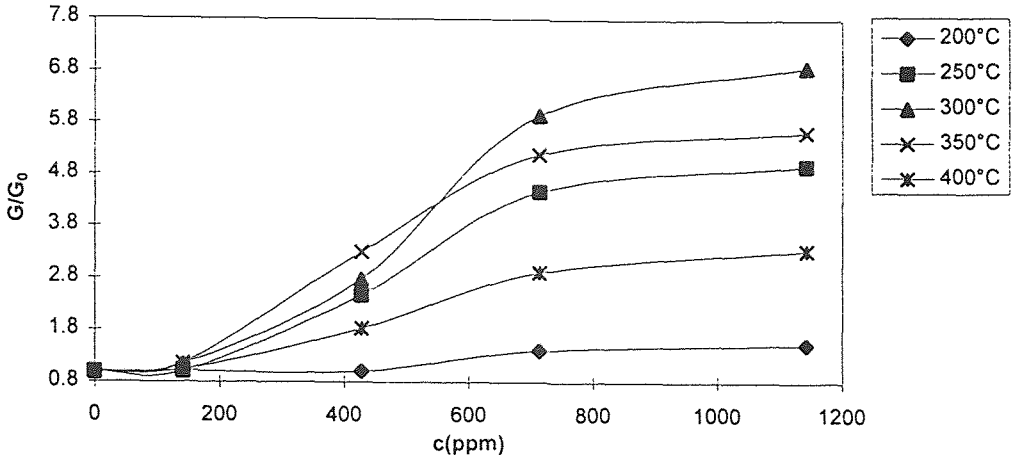

b. SnO_2-Pt sensor

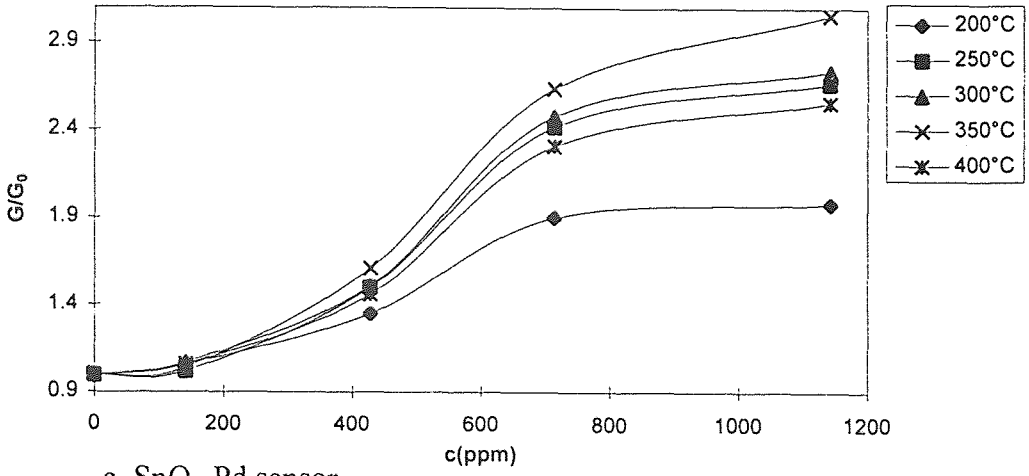

c. SnO_2-Pd sensor

Figure 2.4 Response curves for SnO_2, 450°C gas sensors

SnO_2-Pt sensors present lower ethanol-detection properties. Sensitivity is lower for those sensors and the optimal working temperature is higher. The variation of ethanol-sensing properties with the temperature is different for SnO_2 sensors annealed at 800°C. The average grain size corresponding to this temperature is of 30-70 nm. It was described in the previous section how the grain size is influencing the gas-sensing properties. We can estimate the Debye length (1.27) by using for the concentration of electrons the data presented in Table 1. All donors are assumed to be ionized. For the relative dielectric constant of a ionic crystal, a value of 8 is reasonable. The Debye length is of ≈50 nm. Thus, the average grain size of the SnO_2 for an annealing temperature of 800°C is of the order of the Debye length which means that the predominant conduction mechanism is of hopping over the Surface Schottky barrier. For smaller grain size (450°C annealing temperature) the grains may be completely depleted of majority carriers. The electrons are confined on the grains surface. The conduction mechanism is quite different in this case. It has been shown elsewhere (Barsan, 1994b) that the surface mobility depends on the gas concentration. The conductivity may be obtained in a simple approximation by a formula of the type $g=en\mu$. The mechanism may be, though, much more complex. The surface layer is a highly correlated electron system. Finding a real-space renormalization technique and deriving the electronic energy levels for such a system is an opened problem. In the present work we will study the gas sensing mechanism of SnO_2 with large grain sizes, when hopping over the Schottky barriers seems to best describe the conduction.

In Figure 2.5 one can see the influence of the working temperature on the

sensitivity. The lower the temperature is the higher the sensitivity seems to be. The time of response is however longer at lower temperatures and the value of the conductance is less stable. For all types of sensors, one can observe a long time of response at low temperatures (150°C -200°C). The time of response becomes shorter as the working temperature increases.

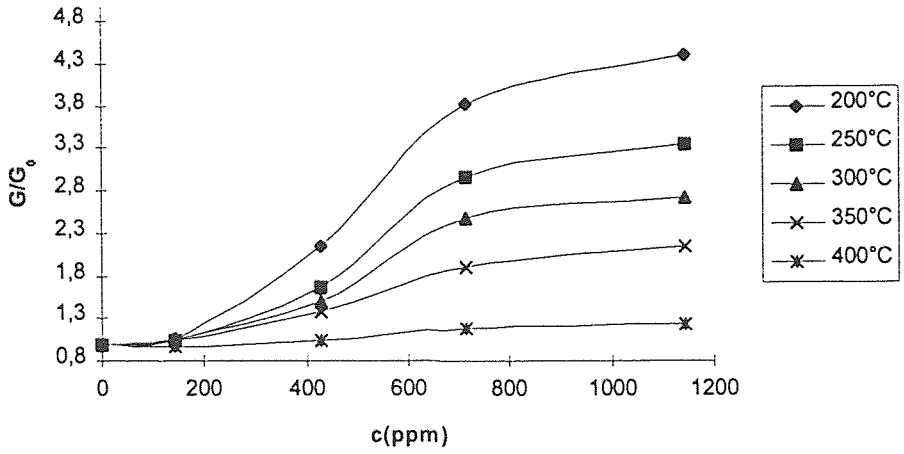

Figure 2.5 Response curves of a SnO_2, 800°C sensor

For elevated temperatures (about 400°C), an extremely quick drop of the resistivity, followed by a slow small variations towards a steady state is observed. A working temperature between 250°C and 350°C (depending on the type of the material, the porosity, the nature of the contacts, etc.) seems to be optimal for ethanol-detection application with SnO_2-based gas sensing devices. The time of response for the tested sensors when exposed from a 400 ppm ethanol atmosphere to a 700 ppm atmosphere, is

represented graphically in Figure 2.6. It is obvious from there that sensors with larger average grain sizes, though less sensitive, have a quicker response to changes of the gas concentration.

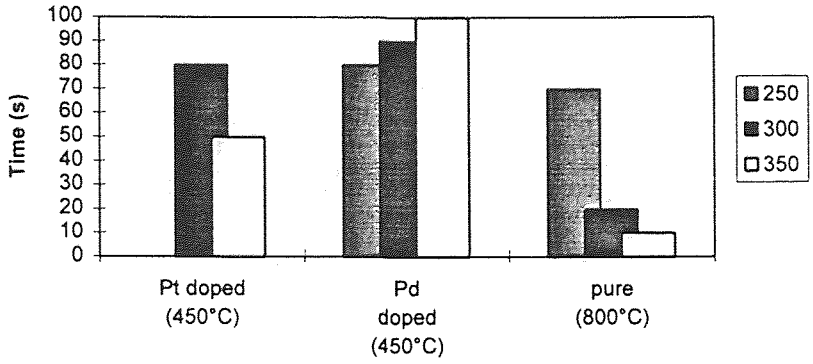

Figure 2.6 Time of response of the sensors

The time of response of the 800°C, SnO_2 sensor when exposed to increasing gas concentration (0 ppm, 140 ppm, 420 ppm, 710 ppm, 1140 ppm) as a function of the working temperature is presented in Figure 2.7.

At low temperatures (150°C), the time of response is much larger than at higher temperatures (of the order of hours) and therefore it was not represented on the graph. One can observe a minimum of the time of response around 350°C. In spite of the decrease of the sensitivity with the increasing temperature, the optimal working temperature for an SnO_2, 800°C sensor for the detection of the ethanol would be around 300°C - 350°C

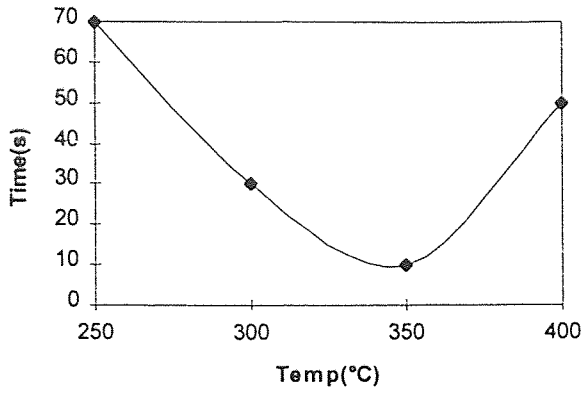

Figure 2.7 Time of response for a SnO_2, 800°C sensor

Of a major importance for the gas-sensing properties is the role of water vapors. In the present work, the water is assumed to have a blocking role for the chemisorption of the oxygen. Surface oxygen vacancies are the sites of atmospheric oxygen adsorption as it was emphasized in the previous sections. The adsorption of oxygen lowers the conductivity by means of 2 mechanisms. First, conduction electrons may be trapped by the adsorbed oxygen species. Adsorbed O^-, also creates a net negative surface charge which induces a depletion layer at the surface. A Schottky-barrier occurs, thus, at the surface. The effect of a reducing gas is precisely to reduce the surface concentration of the adsorbed oxygen and, thus, increase the conductivity. If water vapor is present, it may be adsorbed too on the surface sites (oxygen vacancies). Water may be adsorbed as molecular species or as hydroxyl groups. At elevated temperatures, adsorbed water molecules may also dissociate at the surface. Adsorption of a water molecule has two effects. First, an adsorption site is occupied, thus, the surface coverage with chemisorbed oxygen is lower and the conductivity is higher. Also, a molecule of water doesn't increase

the surface barrier height, because it doesn't carry a net charge. A dipole sheet occurs, thus, at the surface. This affects the surface energy levels. Fluctuation of those levels is a normal occurrence in polar mediums. In the studied case, of sensors with large grain size, one estimate that the predominant effect of adsorbed water is a monopolar one, and consists in the decrease of the net surface charge and the increase of the bulk electron concentration. The ratio of the conductivity of the sensor in clean 100% humidified air and the conductivity in a 30% humidified air is presented in Figure 2.8

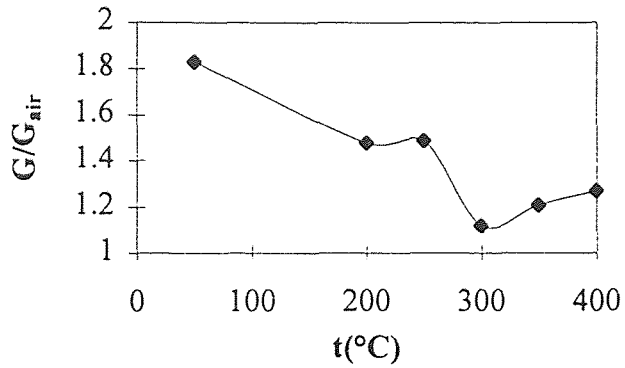

Figure 2.8 Conductivity in 100% humid air

It results from the work of Yamazoe that water molecules are completely desorbed 400°C (Yamazoe et al., 1979). Above this temperature, hydroxyl groups are present at the surface as it can be seen from Figure 2.8. Minimums of the sensitivity correspond to desorption peaks. The two desorption peaks were experimentally observed by a TPD method (Yamazoe et al., 1979). The time of response is shown in Figure 2.9

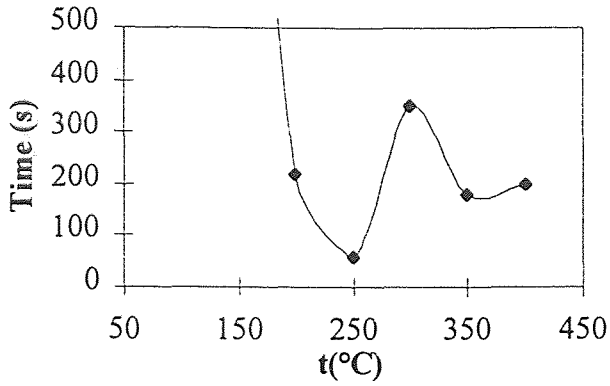

Figure 2.9 Time of response in clean 100% humidified air

At temperatures above 250°C, the response of the sensor when exposed from ambient atmosphere to a humidified one (100%) consists in a quick increase of the conductivity, followed by a very slow decrease towards a steady state. This causes an increase of the time of response as it can be seen from Figure 2.9. This behavior may be due to the adsorption of water in molecular species (which is rapid) followed by the dissociation at the surface into OH^- and H^+ ions. One estimate, thus, that the dissociation of molecular water at the semiconductor surface starts at 250°C.

One can see, in conclusion, that for ethanol-detection purposes, the metallic dopants do not increase dramatically the sensitivity. The SnO_2-Pt sensors have though, a higher sensitivity, but their time of response is higher. For all studied SnO_2-based sensors, the optimal working temperature seems to be around 250°C. Collected data also suggest that sensors with smaller grain sizes have better ethanol-sensing properties. For a complete description of the influence of the dopants and of the porosity on the ethanol-sensing properties, more experimental and theoretical work is needed.

2.2.2 Gas Sensing Mechanisms

In this section, a model of the gas-sensing processes occurring at the tin-oxide surface will be presented. It was emphasized in the previous sections the "sensitizing" role of the adsorption of atmospheric oxygen.

Oxygen is adsorbed as charged species on the surface oxygen vacancies (Yamazoe et. al., 1979), (Barsan, 1994b). It results that associated with the surface oxygen vacancies there are several types of atomic sites:

(a) Oxygen vacancies.

(b) Oxygen vacancies occupied by O^- ions.

(c) Oxygen vacancies occupied by O^{--} ions

(d) Oxygen vacancies occupied with O_2^- ions

The donor states which cause the n-type conductivity are associated with the oxygen vacancies. Numerical values for the oxygen vacancies (donors) concentration are given in Table 1. Associated with (b) and (c) surface sites, there are O^-/O^{--} acceptor states corresponding to the redox process:

$$O^{--} \leftrightarrow O^- + e^-$$

The O^-/O^{--} is represented on the band diagram by an energy level placed in the band gap (Figure 2.10). In our discussion we will assume the active adsorbed species is O^- (Morrison, 1994).

The adsorption of O^- ions from the ambient atmosphere will create the O^-/O^{--} acceptor states and also a surface negative charge distribution. The reducing gas interacts with the

chemisorbed oxygen (Barsan 1993b) and the reaction product is desorbed. As a result, the surface site re-becomes an unoccupied oxygen vacancy (a). Associated with the reduction of oxygen by the reducing gas a donor state RO/RO$^-$ will appear on the band diagram:

$$R+O^- \rightarrow RO + e^-$$

The central idea is to assume the reducing gas molecules are "adsorbed" on pre-adsorbed atmospheric oxygen. The adsorption sites for the oxygen are surface oxygen vacancies or interstitial sites. This method of "conditioned adsorption" allowed us to derive a formula relating the surface coverage of ionic oxygen (O^-) to the partial pressure of the reducing gas. By introducing this formula in equation (1.26), a relation between the Schottky-barrier height and the partial pressure of the reducing gas will be obtained. This modulation of the Schottky-barrier heights by the concentration of the reducing gas is precisely the gas sensing mechanism. Based on this model, theoretical response curves G=G(p) will be plotted after fitting two parameters with the experimental data (surface concentration of adsorption sites for oxygen and surface energy level for the reducing gas)

The first step of the sensing mechanism is thus the "sensitizing" chemisorption of oxygen. Negative-charged O^- ions are adsorbed in various sites (Gopel, 1995). As in the SnO_2 lattice, the oxygen appears as O^-, this adsorption creates surface electronic states, on which conduction electrons will be trapped. Thus, the adsorption of oxygen, lowers the conductivity by increasing the surface-barrier height and by lowering the conduction electrons concentration.

The surface coverage of adsorbed oxygen, according to (1.18) leads to a value for the oxygen coverage close to 1 if one assumes an energy level of the oxygen-traps of 0.5-1 eV. We will assume this coverage ratio to be 1: $\theta_0 \cong 1$. The same result was obtained by Barsan (Barsan, 1994b), starting from the quasichemical equations describing the surface reactions with oxygen and reducing gases.

We will also assume that conduction electrons are trapped on all the adsorbed oxygen species. The effect of the reducing gas is to reduce the chemisorbed oxygen. As a consequence, the surface net charge is lowered and the trapped electrons are released back to the conduction band. Further on we will use the following notations:

- θ_R - surface coverage of reducing gas atmospheres (with respect to the chemisorbed oxygen surface density)
- N_- - surface density of negatively-charged chemisorbed oxygen. The chemisorbed oxygen carries a 2e negative charge due to the capture of a conduction electron
- N_S - Density of surface adsorption sites for oxygen.
- n_0 - concentration of conduction electrons in the absence of the reducing gas.
- N_D - volume concentration of donors (oxygen vacancies)
- x_0 - penetration depth of the band bending (Figure 1.1)

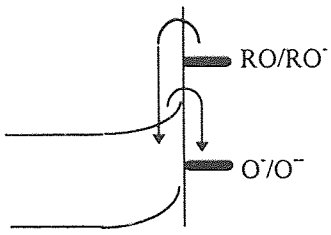

$R+O^- \rightarrow RO+2e^-$
$O^-+e^- \leftrightarrow O^{--}$

Figure 2.10 The band model of the interaction of a reducing gas with adsorbed oxygen

We have then, for the surface density of the chemisorbed oxygen and for the concentration of conduction electrons, in the presence of a reducing gas the relations:

$$N_{-} = N_S \cdot (1 - \theta_R)$$

$$n = n_0 + \frac{2 \cdot \theta_R N_S S}{V}$$

We used the fact that when the oxygen is reduced, two electrons are injected back to the conduction band (see Figure 2.10). The crystallites are assumed to be spheres of radius r. S and V are their surface and volume. The electrons participating at the conduction are those situated in the non-depleted layer. Thus, the apparent electron concentration can be written:

$$n_0 = \frac{N_D (r - x_0)^3}{r^3}$$

The depth x_0 can be derived from the charge conservation law: $x_0 = N_S / N_D$. The concentration of conduction electrons may then be written as:

$$n = n_0 + \eta \theta_R \qquad (2.3)$$

The parameters η and n_0 are given by:

$$n_0 = N_D\left(1-\frac{N_S}{r\cdot N_D}\right)^3 \qquad (2.4)$$

$$\eta = \frac{2\cdot N_S\cdot S}{V}$$

The net surface charge density will be given by:

$$\sigma = 2eN_S\ (1-\theta_R)$$

By introducing this formula into the equation (1.26), one obtains, for the surface Schottky-barrier height:

$$V_S = \frac{2eN_S^{\,2}}{\varepsilon N_D}(1-\theta_R)^2$$

The coverage ratio is related to the partial pressure by the equation (1.18) The barrier height becomes then:

$$V_S = \frac{V_0}{\left(1+\rho\frac{p}{\Pi}\right)^2} \qquad (2.5)$$

V_0 is the barrier height in the absence of the reducing gas:

$$V_0 = \frac{2 \cdot e \cdot N_S^2}{\varepsilon \cdot N_D} \tag{2.6}$$

The conductivity of the sensor will be given by:

$$G = en\mu$$

where μ is the bulk mobility and n the concentration of the electrons. Only those electrons which have enough energy to pass over the barrier height will participate in the conduction process. By using (2.3) and (2.5), the conductivity becomes:

$$G = e\mu \left(n_0 + \eta \frac{\rho \frac{p}{\Pi}}{1 + \rho \frac{p}{\Pi}} \right) e^{-\frac{eV_0}{kT} \frac{1}{1+\rho\frac{p}{\Pi}}}$$

Defining, G_0, the conductivity in clean air as:

$$G_0 = e\mu n_0 e^{-\frac{eV_0}{kT}}$$

one obtains for the sensitivity of the sensor (G/G_0 ratio), the relation:

$$\frac{G}{G_0} = \left(1 + \frac{\eta}{n_0} \cdot \frac{\rho \frac{p}{\Pi}}{1 + \rho \frac{p}{\Pi}}\right) e^{-\frac{eV_0}{kT} \cdot \frac{1}{1+\rho\frac{p}{\Pi}}} \qquad (2.7)$$

In the absence of the reducing gas (p=0), equation (2.7) implies a value for the sensitivity equal to 1. At high pressures, when $\rho(p/\Pi)>>1$, the sensitivity reaches a saturation value:

$$\left.\frac{G}{G_0}\right|_{sat.} = 1 + \frac{\eta}{n_0} \qquad (2.8)$$

The parameters η, n_0 and V_0 are given by (2.4) and (2.6). For the donor concentration appearing in those formulas we will take the value presented in Table 1.(N_D=9.2*10^{21} m^{-3}) For the average radius of the grains, a value of 30nm will be considered. This corresponds to a annealing temperature of 800°C. For determining the surface density of adsorption states, one can assume, these states are the donor sites (oxygen vacancies) which lie within a distance of the order of the lattice constant ($\delta \cong 0.5$ nm for the SnO_2) from the surface. Simple arithmetic manipulations leads to the following expression for N_S:

$$N_S = \frac{N_D R}{3}\left(1 - \frac{3\delta}{R}\right)$$

The numerical value is:

$$N_S \cong 1.48 * 10^{14}\ m^{-2} \qquad (2.9)$$

With this surface density of states, from (2.8), it results a saturation value of 30.

A SnO_2-based sensor annealed at 800°C was tested in very high ethanol pressure. 100 ml of ethanol were dissolved in 2l of water and the mixture was allowed to reach a constant temperature. The concentration of ethanol in the saturated atmosphere is of 201,090 ppm. The experimental value of the sensitivity (G/G_0) in this ethanol concentration (which is considered to be the saturation value) at a working temperature of 300°C is of 100. There are several possible explanations for this result. One can assume than oxygen can be chemisorbed not only on oxygen vacancies as it has been assumed but, also on interstitial sites. One may also assume that the oxygen vacancies concentration is higher at the surface. In both cases the effect is the same: the surface density of adsorption sites is higher than (2.9)

From Figure 2.11, which is obtained by plotting the saturation value of the sensitivity as a function of the surface density of states from (2.8), it can be seen that a value $N_S \cong 2.6 * 10^{14}\ m^{-2}$ leads to a correct value for the saturation sensitivity. The parameter ρ is to be determined now. Note that the fitting of the theoretical equation (2.7) with the experimental values is done for a single temperature - 300°C. Essentially this is because in this treatment we didn't take into considerations variations of the surface coverage of water (or hydroxyl) molecules.

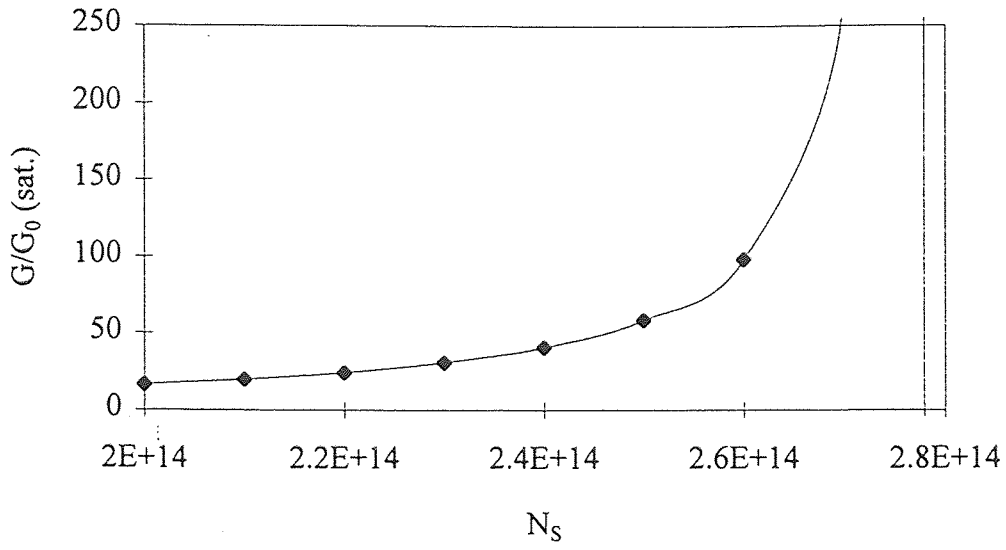

Figure 2.11 Saturation value of the sensitivity as a function of the surface density of adsorption sites

A more complete description of the adsorption processes which occur at the SnO_2 surface, taking into consideration all gaseous species that are present: air (containing oxygen species), reducing gas and water vapors will be presented in a subsequent work.

For the moment one assumes that the surface coverage of water molecules depends more on the temperature than on the concentration of the reducing gas, and this ratio may therefore be considered as constant as long as the temperature is constant. This approximation, however will induce some deviations from the experimental curve.

The shape of the obtained theoretical curve (Figure 2.13) explains why the experimental data is usually fitted by a power low ($G \propto p^n$). This law is referred in the literature as the Sakai law.

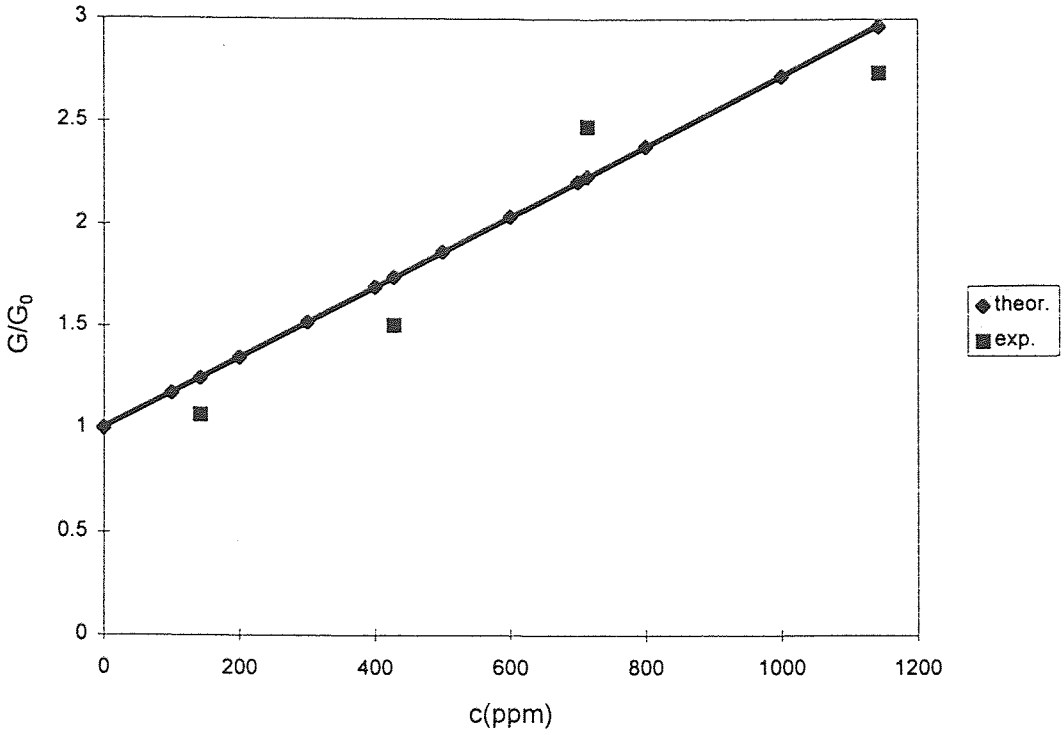

Figure 2.12 Theoretical vs. Experimental response curve of a SnO_2-based gas sensor

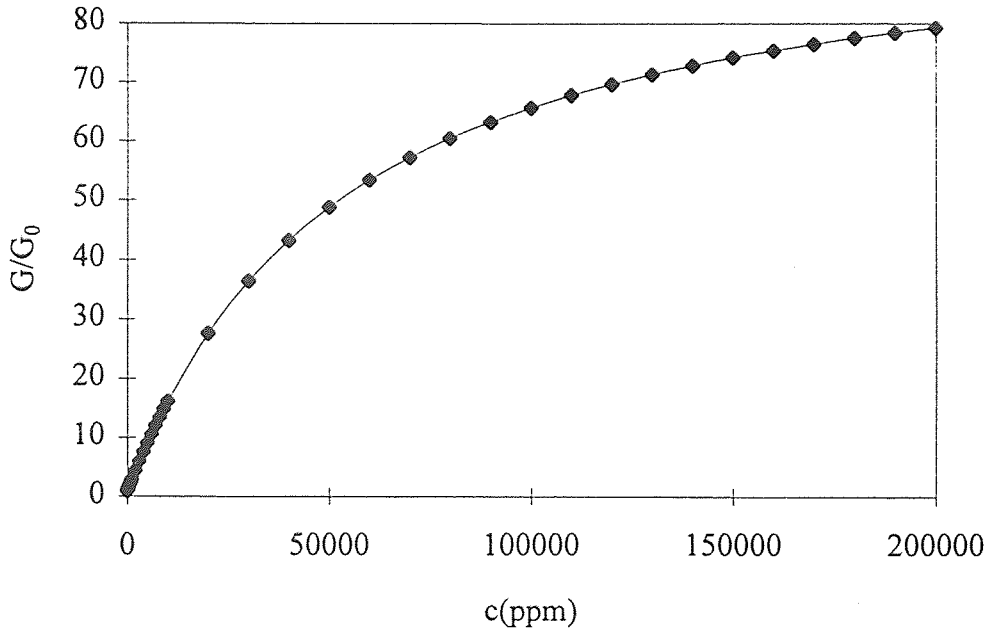

Figure 2.13 Theoretical response curve for a SnO_2 based sensor

From the obtained response function (2.7), as a low-pressure limit a linear dependence $G \propto p$ is obtained. According to previous research (Barsan, 1994b) the exponent appearing in the power low may vary for different species of adsorbed oxygen. Probably a more detailed treatment of the adsorption (section 1.3) will lead to different adsorption isotherms for different species.

The most obvious improvements of this model are, in the opinion of the author, to take into considerations of the role of water vapors in the adsorption as a concurrent adsorption to the oxygen chemisorption, and to take into consideration the role of holes in the conduction mechanism (Barsan, 1989). Also, by taking into consideration the adsorption mechanisms and the corresponding reduction reaction for different species of atmospheric oxygen, the results may be improved. .

CHAPTER 3

CONCLUSIONS

In this thesis we have accomplished the following research work:

- Several measurements of conductance and time of response of thick-film devices have been performed for the case of pure SnO_2 as well as for samples with catalysts (Pt and Pd). Experimental results were obtained both by varying the temperature at fixed ethanol concentration or by varying the ethanol concentration at fixed temperature. All measurements were done in wet, 100% relative humidity, atmospheres. The experimental data show a dependence of the ethanol sensing properties as a function of the structure of the sensing material. The working temperature and the average grain size have been found to have a major importance for the sensitivity of the SnO_2-based gas sensors upon variation of ethanol concentrations.

- A qualitative model of the influence of the water vapors on the sensor conductivity is proposed in section 2.2.1. This model assumes that the adsorption of water as molecular species or as hydroxyl species can be done on the surface oxygen vacancies. This assumption allowed us to explain the influence of the non-dissociated water molecules on the conductivity of the SnO_2 film. Based on the experimental data, one estimates that the dissociation of water molecules at the semiconductor surface starts at temperatures around 250°C. The important influence of the humidity on the conductance of the sensors at working temperatures below this temperature is considered to be an experimental proof of the influence of water molecules. One estimate also that

the dipolar field associated with the polar molecules (water) has an important effect on the conductivity of materials with small grain sizes. More experimental and theoretical work is, however, needed for presenting a complete picture of the role of water molecules on the electrical conductivity of such sensing layers.

- In section 2.2.2 we presented a theoretical model of the gas sensing mechanisms in SnO_2 films with grain sizes comparable to or larger than the Debye length. The model accepts the conduction mechanism as being governed by the Schottky barriers which occur at the grain interfaces. For obtaining the surface coverage of the semiconductor with charged oxygen species (O^-), a method, of "conditioned adsorption" was developed. The central idea was to assume that the reducing gas molecules are "adsorbed" (i.e. react) only on pre-adsorbed oxygen. This approach allowed us to avoid the use of the quasichemical equations of the reactions which occur at the SnO_2 surface. The number of parameters which were introduced to fit the theoretical curves with the experimental results was thus reduced. The total elimination of the parameters was however not possible. Values for the "adsorption energy" of the reducing gas and for the surface density of adsorption sites for atmospheric oxygen were obtained after fitting the theoretical equations with the experimental data. The predictions made in the frame of the presented theoretical model are in good agreement with the experimental data. The proposed model also predicts the decrease of the sensitivity with the increasing working temperature. Experimentally, this behavior is clearly proved in Figure 2.5.

REFERENCES

Barsan, N.; Grigorovici, R.; Ionescu, R,; Motronea, M. and Vancu, A. (1989), "Mechanism of Gas Detection in Polycrystalline Thick Film SnO_2 Sensors", *Thin Solid Films* **171**, 53

Barsan, N. and Ionescu,R.(1993a) "The Mechanism of the Interaction between CO and an SnO_2 Surface: The Role of Water Vapor", *Sensors and Actuators* B12, 71-75

Barsan, N. (1993b), *Non Equilibrium Phenomena at the Interface Gas-Oxidic Semiconductor*, Ph.D. Thesis, University of Bucharest, Magurele, Romania

Barsan, N., Ionescu,R., Vancu,A. (1994a), "Calibration Curve fir SnO_2-based Gas Sensors", *Sensors and Actuators* **B18-19**, 466-469

Barsan, N. (1994b), "Conduction Models in Gas-Sensing SnO_2 Layers: Grain-Size Effects and Ambient Atmosphere Influence", *Sensors and Actuators* **B17**, 241-246

Frankl, Daniel R. (1967) *International Series of Monographs on Semiconductors v.7 Electrical Properties of Semiconductor Surfaces*. Oxford, New York: Pergamon Press

Gopel, Wolfgang, Schierbaum,Klaus Dieter (1995), "SnO_2 Sensors: Current Status and Future Prospects", *Sensors and Actuators* **B26-27**, 1-12

Jarzebski, Z.M. and Marton, J.P. (1976), "Physical Properties of SnO_2 Materials - Electrical Properties", *J. Electrochem. Soc.* 123 No.9, 299C-310C

Kohnke, E.E.(1962), *J. Phys. Chem. Solids* 23, 1557

Maier, J. and Gopel, W. (1988), *J. Solid State Chem* 72, 293

Martinelli, G., Carotta,M.C. (1995), "Thick-Film Gas Sensors", *Sensors and Actuators* B23, 157-161

McAleer, J.F.; Moseley, P.T.; Norris J.O.W. and Williams D.E. (1987), "Tin Dioxide Gas Sensors part I, Aspects of the Surface Chemistry Revealed by Electrical Conductance Variation", *J.Chem.Soc. Faraday Trans.* 1 83, 1323-1346

McQuarrie, D.A. (1976) *Statistical Thermodynamics*. New York: Harper & Row

Mizsei, J. (1995), "How Can Sensitive and Selective Semiconductor Gas Sensors be Made?", *Sensors and Actuators* B23, 173-176

Morrison, S.Roy (1977) *The Chemical Physics of Surfaces.* New York: Plenum Press

Morrison, S.Roy (1982), "Semiconductor Gas Sensors", *Sensors and Actuators* 2, 329-341

Morrison, S.Roy (1987), "Selectivity in Semiconductor Gas Sensors", *Sensors and Actuators* 12, 425-440

Morrison, S.Roy (1994) in *Semiconductor Sensors,* Sze, S.M. ed., Chap.8: Chemical Sensors, New York: John Wiley & Sons

Schweizer-Berberich, M.; Zheng, J.G.; Weimar, U.; Gopel,W.; Barsan,N.; Pentia, E; Tomescu,A. (1996), "The Effect of Pt and Pd Surface Doping on the Response of Nanocrystalline Tin Dioxide Gas Sensors to CO", *Sensors and Actuators*, B 31, 71-75

Yamazoe, N. (1991), "New Approaches for Improving Semiconductor Gas Sensors", *Sensors and Actuators* B5, 7-19

Yamazoe, N.; Fuchigami, J.; Kishikawa, M. and Seiyama, T. (1979), "Interaction of Tin Oxide with O_2, H_2O and H_2", *Surface Science* 86, 335-344